# Supporting Information

# H-Type-like Aggregation-Accelerated Singlet Fission Process in Dipyrrolonaphthyridinedione Thin Film: The Role of Charge Transfer/Excimer Mixed Intermediate State

Long Wang,[1*†] Wanlin Cai,[2†] Jing Sun,[1] Yuling Wu,[1] Bin Zhang,[2] Xiangbin Tian,[1] Shaoting Guo,[1] WanZhen Liang,[2*] Hongbing Fu,[3] and Jiannian Yao[4]

[1] *Key Laboratory of Interface Science and Engineering in Advanced Materials, Ministry of Education, Taiyuan University of Technology, Taiyuan 030024, China*

[2] *Department of Chemistry, College of Chemistry and Chemical Engineering, Xiamen University, Xiamen 361005, China*

[3] *Beijing Key Laboratory for Optical Materials and Photonic Devices, Department of Chemistry, Capital Normal University, Beijing 100048, China*

[4] *Key Laboratory of Photochemistry, Institute of Chemistry, Chinese Academy of Sciences, Beijing 100190, China*

Corresponding Authors:

* L. W., email: wanglong@tyut.edu.cn, W.-Z. L., email: liangwz@xmu.edu.cn.

† These authors contributed equally to this work.

## Table of Contents

**1. Materials and Methods**.

$^{1}$H-NMR and $^{13}$C-NMR spectra were recorded on a Bruker Avance 300 spectrometer using the solvent peak as the reference standard, with chemical shifts given in parts per million. Dichloromethane-d2 ($CD_2Cl_2$) was used as NMR solvent. MALDI-TOF mass spectra were recorded on Bruker Ultrafre Xtreme.

**Sample Preparation.** Single crystal was grown by the vapor diffusion of methanol (poor solvent) into a chloroform solution (good solvent). Pure thin films were prepared by vacuum deposition technique on sapphire or quartz substrate at a rate of 0.3 Å/s under a vacuum of $10^{-5}$ mbar.

**Steady-State Spectroscopic Measurements.** UV-visible absorption and fluorescence spectra were measured on Shimadzu UV-3600 spectrometer and Hitachi F-4500 spectrophotometer, respectively. X-ray diffraction (XRD) patterns of the thin films were carried out in the reflection mode at room temperature using a 2 kW Rigaku XRD system.

**Time-Resolved Spectroscopy Measurements and Kinetic Analysis.** Time-resolved photoluminescence spectra were detected by FLS980 spectrometer equipped with an EPL-375 picosecond pulsed diode laser (Edinburgh Instruments Ltd.). Femtosecond transient absorption (fs-TA) and nanosecond transient absorption (ns-TA) spectroscopy measurements were all performed using previously described instruments and experimental conditions.[1-2] Analysis of the kinetic traces derived from time-resolved spectra was performed individually and globally using nonlinear least-square fitting to a general sum-of-exponentials function after de-convolution of instrument response function (IRF). Species associated kinetic analyses of fs-TA data were performed using singular value decomposition (SVD) followed by global fitting performed using lab-written MATLAB programs. The data for thin film samples were fit to the following sequential four-state kinetic model ($A \rightarrow B \rightarrow C \rightarrow D \rightarrow S_0$)[3-4]:

$$\frac{d[\mathrm{A}]}{dt} = -k_1[\mathrm{A}];\ \frac{d[\mathrm{B}]}{dt} = k_1[\mathrm{A}] - k_2[\mathrm{B}];$$

$$\frac{d[\mathrm{C}]}{dt} = k_2[\mathrm{B}] - k_3[\mathrm{C}];\ \frac{d[\mathrm{D}]}{dt} = k_3[\mathrm{C}] - k_4[\mathrm{D}]$$

## 2. Molecular Synthesis.

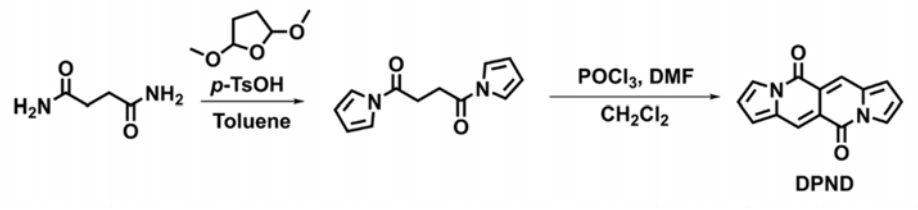


**Scheme S1**. Synthetic route of **DPND** molecule.

The intermediate 1,4-di(pyrrol-1-yl)butane-1,4-dione and the desired compound **DPND** were synthesized according to the literature with some minor modifications in the purification procedures (**Scheme S1**).[2, 5] Under an argon atmosphere, to the solution of the intermediate (432 mg, 2.0 mmol) in 10 mL of dry $CH_2Cl_2$, DMF (0.39 mL, 5.0 mmol) was added. Then $POCl_3$ (0.48 mL, 5.2 mmol) was added dropwise and the mixture was refluxed for 2 h. The reaction was quenched by the addition of saturated aqueous $NaHCO_3$ solution, and then extracted by $CH_2Cl_2$ and water. The combined organic layers were washed with water, brine, and dried over $Na_2SO_4$. The recrystallization procedure was performed by slow addition of MeOH to a solution of the crude product in small amount of $CH_2Cl_2$. Then product was purified using column chromatography (silica, hexanes: $CH_2Cl_2$ 2:1 to 1:1). Compound **DPND** (45 mg, 9.6% yield) was obtained as a brown powder.

**5H,11H-dipyrrolo[1,2-b:1',2'-g][2,6]naphthyridine-5,11-dione** (**DPND**): $^1$H NMR (300 MHz, $CD_2Cl_2$) δ: 7.86 (s, 2H), 7.71-7.72 (m, 2H), 6.74-6.75 (m, 2H), 6.45-6.48 (m, 2H). $^{13}$C NMR (75 MHz, $CD_2Cl_2$) δ: 158.2, 131.4, 124.9, 123.3, 118.2, 116.0. HRMS (MALDI-TOF) Calculated for $C_{14}H_9N_2O_2^+$: 237.0659, found: m/z 237.0584.

**3. Molecular Arrangements in Single Crystal.**

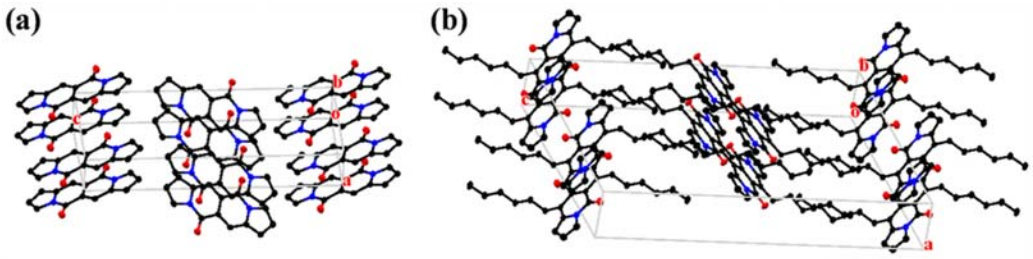


**Figure S1**. Molecular arrangements in single crystal cells of **DPND** and **DPND6**.

**4. Fluorescence Property.**

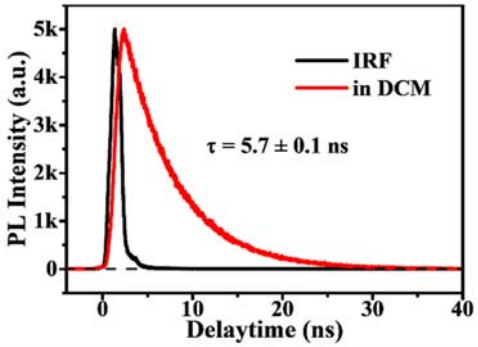


**Figure S2**. Transient PL decay curve (537 nm) of **DPND** molecule in dilute $CH_2Cl_2$ solution.

**5. Phosphorescence Data.**

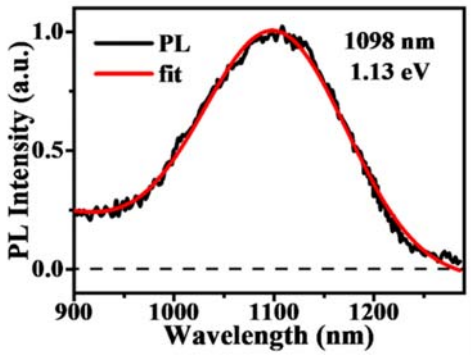


**Figure S3**. Steady state NIR emission spectra of Pt(TPBP) doped **DPND** thin film at 77 K. PtTPBP has reported to be a good triplet sensitizer with a long triplet lifetime of ~42 μs.[2] Sample was prepared by spinning THF solutions of **DPND**, and the sensitizer with a weight ratio of 95:5. The phosphorescence spectra exhibit emission peak at 1098 nm indicating a triplet energy of 1.13 eV for **DPND** molecule in aggregated states.

## 6. Theoretical Methods and Computational Details.

### 6.1 Computational Details.

The molecular ground-state geometry optimizations and frequency calculations were performed by the density functional theory (DFT) with exchange-correlation (XC) functional PBE0-D3BJ[6-8] and 6-311G** basis set within the Gaussian 16 program package.[9] The first singlet ($S_1$) and triplet ($T_1$) excited states were obtained by the time-dependent DFT (TDDFT) approach and unrestricted DFT method, respectively,[10] and the tuned long-range-corrected XC functional LC-PBE0 with def2-TZVP basis were used to refine the excitation energy.[11] The environmental effects of **DPND** and **DPND6** aggregates were embodied via the polarizable continuum model (PCM). Here, the dielectric constant $\varepsilon$ was evaluated by using the Clausius–Mossotti relation,

$$\frac{\varepsilon - 1}{\varepsilon + 2} = \frac{4\pi}{3}\frac{\alpha}{V}$$

where $\alpha$ and $V$ are the polarizability and the volume of a single molecule, respectively.[12-13] The molecular volume was obtained by using the Multiwfn program.[14] The dielectric constants of **DPND** and **DPND6** aggregates were thus set to 3.4 and 4.6, respectively.

To describe the SF process in a dimer system, we adopt a five-configuration model, in which electronic Hamiltonian includes five diabatic electronic states (two singlet excited (SE) states ($S_0S_1$ and $S_1S_0$), two intermolecular CT states (CA and AC) and one triplet pair (TT) state) and their couplings (**Figure S4**). The electronic coupling ($V_{ex}$) between two SE states and excitation energies of SE and CT states were calculated by using the fragment particle hole densities (FPHD) method,[15] in which the adiabatic-to-diabatic unitary transformation matrix was obtained by localizing the particle and hole densities. The electronic couplings of CT-SE and CT-TT (i.e. $V_{HH}$, $V_{LL}$, $V_{LH}$, $V_{HL}$) were calculated at the PW91PW91/TZ2P level within the ADF program,[16] and two-electron couplings of SE-TT (i.e.$V_{2e}$) were obtained from the four-electron, four-orbital model.[17] To describe SF dynamics taking place in organic molecular aggregates, we incorporate the molecular electron-vibrational interaction. The nuclei vibrations were identified by a collection of harmonic oscillators. SF dynamics were simulated by the time-dependent wavepacket diffusion (TDWPD) method.[18-19] The kernel concept of TDWPD method is very similar to that of stochastic Schrödinger equation

where the molecular vibrational motions are incorporated with random fluctuations on electronic states.

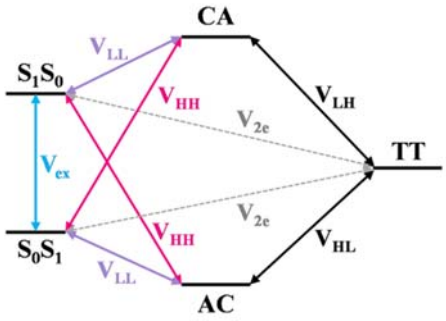


**Figure S4**. The diabatic electronic states and the couplings between these electronic states for dimer.

### 6.2 Model Hamiltonian and TDWPD method.

The total Hamiltonian of oligomer with *N* monomers in one-dimensional molecular chain can be represented as

$$\hat{H}=\hat{H}_{\mathrm{e}}+\hat{H}_{\mathrm{ph}}+\hat{H}_{\mathrm{e\text{-}ph}}, \tag{S1}$$

where $\hat{H}_{\mathrm{e}}$, $\hat{H}_{\mathrm{ph}}$ and $\hat{H}_{\mathrm{e\text{-}ph}}$ are the electronic, phonon and electron-phonon interaction Hamiltonian. The electronic Hamiltonian including singlet exciton (SE), charge transfer (CT), and triplet pair (TT) states can be written as the sum of follows,

$$\begin{aligned}
\hat{H}_{\mathrm{e}} &= \hat{H}_{\mathrm{ex}}+\hat{H}_{\mathrm{CT}}+\hat{H}_{\mathrm{TT}}+\hat{H}_{\mathrm{int}} \\
&=\sum_n E_{\mathrm{ex}}\left|\mathrm{S}_n\right\rangle\left\langle\mathrm{S}_n\right|+\sum_n E_{\mathrm{CT}}\left(\left|\mathrm{A}_n;\mathrm{C}_{n+1}\right\rangle\left\langle\mathrm{A}_n;\mathrm{C}_{n+1}\right|+\left|\mathrm{C}_n;\mathrm{A}_{n+1}\right\rangle\left\langle\mathrm{C}_n;\mathrm{A}_{n+1}\right|\right) \\
&+\sum_n E_{\mathrm{TT}}\left|T_n;T_{n+1}\right\rangle\left\langle T_n;T_{n+1}\right| \\
&+\sum_n V_{\mathrm{ex}}\left(\left|\mathrm{S}_n\right\rangle\left\langle\mathrm{S}_{n+1}\right|+h.c.\right)+\sum_n V_{\mathrm{ex}}^{13}\left(\left|\mathrm{S}_n\right\rangle\left\langle\mathrm{S}_{n+2}\right|+h.c.\right) \\
&+\sum_n V_{\mathrm{HH}}\left(\left|\mathrm{S}_n\right\rangle\left\langle\mathrm{A}_n;\mathrm{C}_{n\pm1}\right|+h.c.\right)+\sum_n V_{\mathrm{LL}}\left(\left|\mathrm{S}_n\right\rangle\left\langle\mathrm{C}_n;\mathrm{A}_{n\pm1}\right|+h.c.\right) \\
&+\sum_n V_{\mathrm{HL}}\left(\left|\mathrm{A}_n;\mathrm{C}_{n+1}\right\rangle\left\langle\mathrm{T}_n;\mathrm{T}_{n+1}\right|+h.c.\right)+\sum_n V_{\mathrm{LH}}\left(\left|\mathrm{C}_n;\mathrm{A}_{n+1}\right\rangle\left\langle\mathrm{T}_n;\mathrm{T}_{n+1}\right|+h.c.\right) \\
&+\sum_n V_{2\mathrm{e}}\left(\left|\mathrm{S}_n\right\rangle\left\langle\mathrm{T}_n;\mathrm{T}_{n\pm1}\right|+h.c.\right)+\sum_n V_{\mathrm{CT}}\left(\left|\mathrm{A}_n;\mathrm{C}_{n+1}\right\rangle\left\langle\mathrm{C}_n;\mathrm{A}_{n+1}\right|+h.c.\right)
\end{aligned} \tag{S2}$$

where $\left|\mathrm{S}_n\right\rangle$ represents that the *n*-th monomer is in the singlet excited state and the others are in the ground state; $\left|\mathrm{A}_n;\mathrm{C}_{n+1}\right\rangle$, $\left|\mathrm{C}_n;\mathrm{A}_{n+1}\right\rangle$ and $\left|\mathrm{T}_n;\mathrm{T}_{n+1}\right\rangle$ represent the *n*-th and (*n*+1)-th monomers are

in the correspond electronic state (cationic (C), anionic (A) and triplet (T) states). The phonon and the electron-phonon coupling Hamiltonians can be written as

$$\hat{H}_{ph} = \sum_n \sum_k \hbar\omega_k \left( \hat{a}_{nk}^{\dagger} \hat{a}_{nk} + 1/2 \right) \tag{S3}$$

$$\hat{H}_{e-ph} = \sum_n \sum_k \hbar\omega_k \left( \hat{a}_{nk}^{\dagger} + \hat{a}_{nk} \right) \otimes \hat{x}_{nk} \tag{S4}$$

$$\begin{aligned} \hat{x}_{nk} = {} & \xi_{\mathrm{S}} \left| \mathrm{S}_n \right\rangle \left\langle \mathrm{S}_n \right| + 2\xi_{\mathrm{T}} \left| \mathrm{T}_n ; \mathrm{T}_{n+1} \right\rangle \left\langle \mathrm{T}_n ; \mathrm{T}_{n+1} \right| \\ & + \xi_{\mathrm{A}} \left( \left| \mathrm{A}_n ; \mathrm{C}_{n+1} \right\rangle \left\langle \mathrm{A}_n ; \mathrm{C}_{n+1} \right| + \left| \mathrm{C}_n ; \mathrm{A}_{n+1} \right\rangle \left\langle \mathrm{C}_n ; \mathrm{A}_{n+1} \right| \right) \\ & + \xi_{\mathrm{C}} \left( \left| \mathrm{A}_n ; \mathrm{C}_{n+1} \right\rangle \left\langle \mathrm{A}_n ; \mathrm{C}_{n+1} \right| + \left| \mathrm{C}_n ; \mathrm{A}_{n+1} \right\rangle \left\langle \mathrm{C}_n ; \mathrm{A}_{n+1} \right| \right) \end{aligned} \tag{S5}$$

where $\xi_{\mathrm{S(A,C,T)}}$ denotes the electron-phonon coupling strength; what is more, $\xi$ is determined by the spectral density $J_n(\omega) = \pi \sum_j C_{nj}^2 \delta(\omega - \omega_{nj})$ in SF dynamics. With the model Hamiltonian in hand, the SF dynamics can be simulated by solving the time-dependent stochastic Schrödinger equation[19-20]

$$i \frac{\partial \left| \psi(t) \right\rangle}{\partial t} = \left( H_e + F_n(t) - iL \int_0^t d\tau \alpha_n(\tau) e^{-iH_e\tau} L e^{iH_e\tau} \right) \left| \psi(t) \right\rangle \tag{S6}$$

where $\alpha_n(t) = \sum_j C_{nj}^2 e^{-i\omega_{nj}t}$ is the zero temperature correlation function of electronic-phonon couplings and $L = \sum_{nm}^{N} |n\rangle\langle m|$. The stochastic force can be written as

$$F_n(t) = \sum_k \sqrt{\frac{J_n(\omega_k)\Delta\omega}{\pi}} \left[ \sqrt{A(\omega_k)} \cos(\omega_k t + \phi_k) + i \sqrt{B(\omega_k)} \sin(\omega_k t + \phi_k) \right] \tag{S7}$$

where $A(\omega_k) = \coth(\omega_k / 2k_{\mathrm{B}}T) + \operatorname{csch}(\omega_k / 2k_{\mathrm{B}}T)$, $B(\omega_k) = \coth(\omega_k / 2k_{\mathrm{B}}T) - \operatorname{csch}(\omega_k / 2k_{\mathrm{B}}T)$ and $\phi_k$ is uniformly distributed in $[0, 2\pi]$. The wave function in the extended TDWPD method can be expressed as $|\psi(t)\rangle = \sum_n c_n(t) |n\rangle$; thus, the population $\rho_{nn}(t)$ can be evaluated by $\rho_{nn}(t) = \left\langle c_n^*(t) c_n(t) \right\rangle$.

### 6.3 The SF dynamics of dimers.

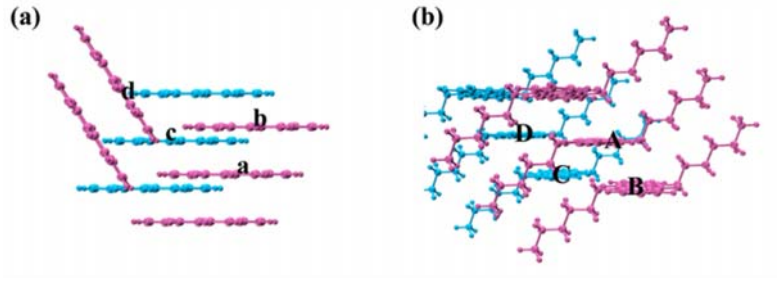


**Figure S5**. Selected dimer units of **DPND** (a) and **DPND6** (b) from single crystal structures.

The corresponding electronic Hamiltonian of the dimer systems has the following matrix form in **eq S8**,

$$H_{\mathrm{e}} = \begin{pmatrix} E_{\mathrm{S_1S_0}} & V_{\mathrm{ex}} & V_{\mathrm{LL}} & V_{\mathrm{HH}} & V_{2e} \\ V_{\mathrm{ex}} & E_{\mathrm{S_0S_1}} & V_{\mathrm{HH}} & V_{\mathrm{LL}} & V_{2e} \\ V_{\mathrm{LL}} & V_{\mathrm{HH}} & E_{\mathrm{CA}} & V_{\mathrm{CT}} & V_{\mathrm{LH}} \\ V_{\mathrm{HH}} & V_{\mathrm{LL}} & V_{\mathrm{CT}} & E_{\mathrm{AC}} & V_{\mathrm{HL}} \\ V_{2e} & V_{2e} & V_{\mathrm{LH}} & V_{\mathrm{HL}} & E_{\mathrm{TT}} \end{pmatrix} \qquad \textbf{(S8)}$$

Then the calculated electronic Hamiltonians (in meV) for the dimer ab, ac, ad, and cd of **DPND**, and AB, AC, AD and BD of **DPND6** (**Figure S5**) are provided in **eq S9-S16**, respectively. The parameters for electron-phonon coupling are provided in **Figure S6** and **S7.** Their corresponding population dynamics and fitting SF rates are presented in **Figure S8** and **Table S1**.

$$H_{\mathrm{ab}} = \begin{pmatrix} 2510.0 & 134.9 & -7.3 & 195.9 & -4.1 \\ 134.9 & 2510.0 & 195.9 & -7.3 & 4.1 \\ -7.3 & 195.9 & 2613.7 & -1.2 & -98.6 \\ 195.9 & -7.3 & -1.2 & 2613.7 & 98.6 \\ -4.1 & 4.1 & -98.6 & 98.6 & 2080.8 \end{pmatrix} \qquad \textbf{(S9)}$$

$$H_{\mathrm{ac}} = \begin{pmatrix} 2510.0 & 71.8 & 13.7 & -16.4 & 0.0 \\ 71.8 & 2510.0 & -16.4 & 13.7 & 0.0 \\ 13.7 & -16.4 & 3345.8 & 0.0 & 4.1 \\ -16.4 & 13.7 & 0.0 & 3345.8 & -4.1 \\ 0.0 & 0.0 & 4.1 & -4.1 & 2080.8 \end{pmatrix} \quad \textbf{(S10)}$$

$$H_{\mathrm{ad}} = \begin{pmatrix} 2510.0 & -36.9 & 4.7 & -2.8 & 0.0 \\ -36.9 & 2510.0 & -2.8 & 4.7 & 0.0 \\ 4.7 & -2.8 & 3910.6 & 0.0 & 2.2 \\ -2.8 & 4.7 & 0.0 & 3910.6 & 4.4 \\ 0.0 & 0.0 & 2.2 & 4.4 & 2080.8 \end{pmatrix} \quad \textbf{(S11)}$$

$$H_{\mathrm{cd}} = \begin{pmatrix} 2510.0 & -43.2 & -7.2 & -6.6 & 0.0 \\ -43.2 & 2510.0 & -6.6 & -7.2 & 0.0 \\ -7.2 & -6.6 & 3928.8 & 0.0 & 8.4 \\ -6.6 & -7.2 & 0.0 & 3928.8 & 5.6 \\ 0.0 & 0.0 & 8.4 & 5.6 & 2080.8 \end{pmatrix} \quad \textbf{(S12)}$$

$$H_{\mathrm{AB}} = \begin{pmatrix} 2546.7 & 100.0 & -4.9 & -34.4 & -2.5 \\ 100.0 & 2546.7 & -34.4 & -4.9 & 2.5 \\ -4.9 & -34.4 & 2726.0 & -0.7 & -96.3 \\ -34.4 & -4.9 & -0.7 & 2726.0 & 96.3 \\ -2.5 & 2.5 & -96.3 & 96.3 & 2415.1 \end{pmatrix} \quad \textbf{(S13)}$$

$$H_{\mathrm{AC}} = \begin{pmatrix} 2546.7 & -37.2 & -46.2 & -53.9 & 0.0 \\ -37.2 & 2546.7 & -53.9 & -46.2 & 0.0 \\ -46.2 & -53.9 & 3549.0 & 0.0 & -51.7 \\ -53.9 & -46.2 & 0.0 & 3549.0 & -51.7 \\ 0.0 & 0.0 & -51.7 & -51.7 & 2415.1 \end{pmatrix} \quad \textbf{(S14)}$$

$$H_{\mathrm{AD}} = \begin{pmatrix} 2546.7 & -11.8 & 19.6 & 15.2 & 0.0 \\ -11.8 & 2546.7 & 15.2 & 19.6 & 0.0 \\ 19.6 & 15.2 & 3616.8 & 0.0 & 17.5 \\ 15.2 & 19.6 & 0.0 & 3616.8 & 17.5 \\ 0.0 & 0.0 & 17.5 & 17.5 & 2415.1 \end{pmatrix} \quad \textbf{(S15)}$$

$$H_{\mathrm{BD}} = \begin{pmatrix} 2546.7 & 9.1 & 0.3 & -0.7 & 0.0 \\ 9.1 & 2546.7 & -0.7 & 0.3 & 0.0 \\ 0.3 & -0.7 & 3998.4 & 0.0 & -0.3 \\ -0.7 & 0.3 & 0.0 & 3998.4 & -0.3 \\ 0.0 & 0.0 & -0.3 & -0.3 & 2415.1 \end{pmatrix} \quad \textbf{(S16)}$$

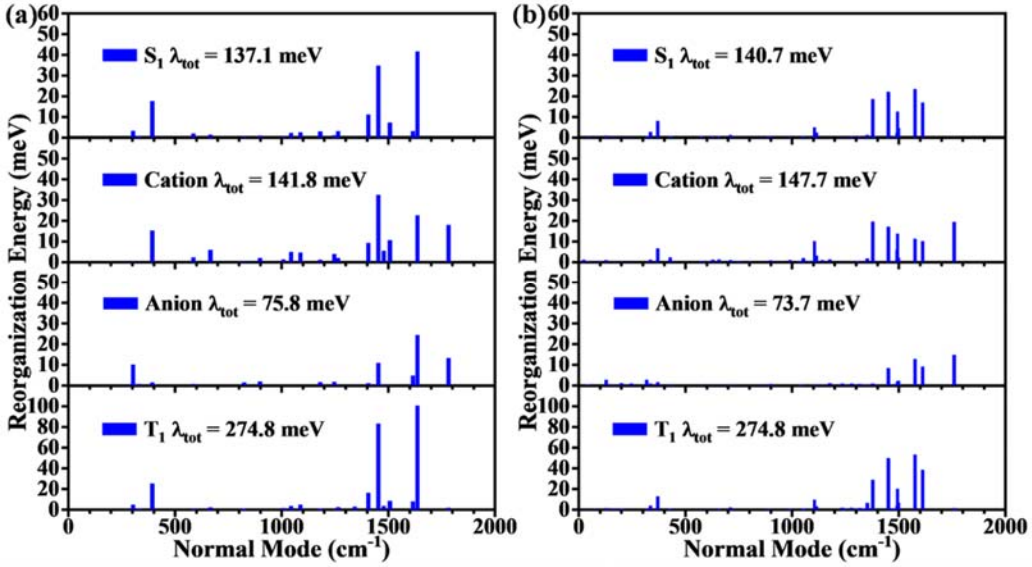


**Figure S6**. Calculated reorganization energy of $S_1$, Cation, Anion and $T_1$ states for a) **DPND** and b) **DPND6** system.

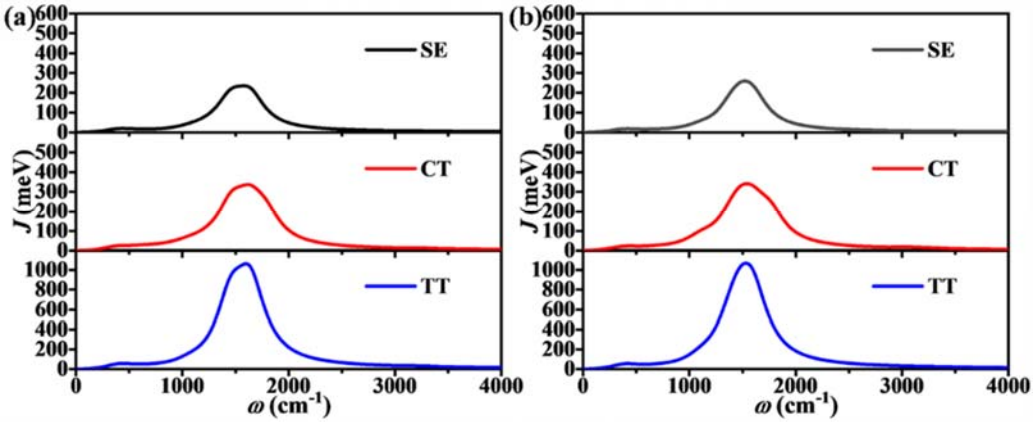


**Figure S7**. Calculated spectral density of SE, CT and TT states for a) **DPND** and b) **DPND6** system.

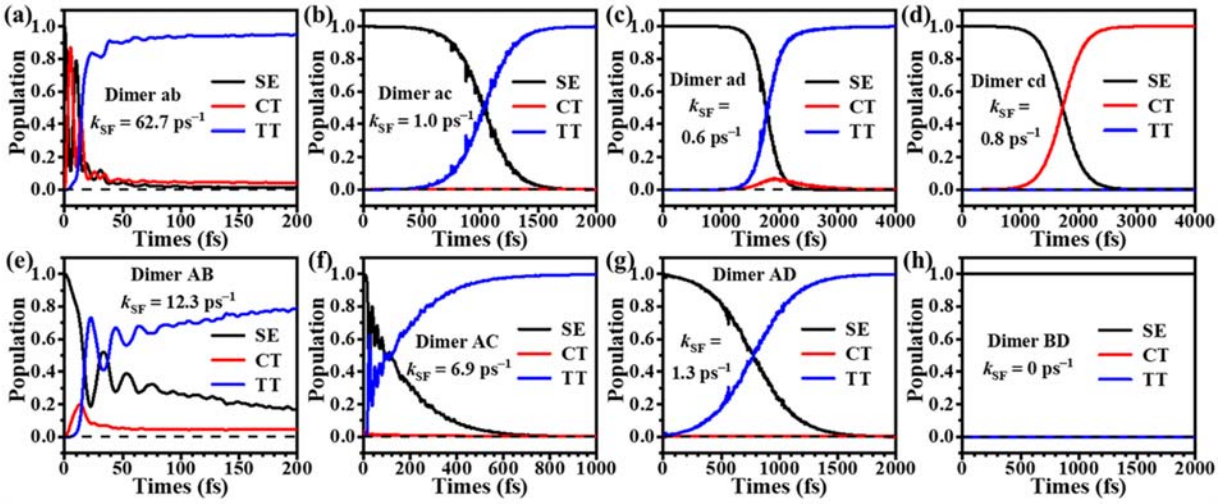


**Figure S8**. Population evolution in SE, CT and TT states for **DPND** and **DPND6** dimers.

**Table S1**. The fitted SF rate (ps$^{-1}$) of the selected dimer units for **DPND** and **DPND6**.

| **DPND** | | | | **DPND6** | | | |
|---|---|---|---|---|---|---|---|
| **ab** | **ac** | **ad** | **cd** | **AB** | **AC** | **AD** | **BD** |
| 62.7 | 1.0 | 0.6 | 0.8 | 12.3 | 6.9 | 1.3 | 0.0 |

Note: The TT state population of Dimer AB, AC and ab were fitted by a two exponential decay function $P$ (TT) = $A_1e^{-t/\tau1} + A_2e^{-t/\tau2} + P_0$; and the SF rate can be defined as $1/\tau$, where $\tau = (A_1\tau_1 + A_2\tau_2) / (A_1 + A_2)$. The $\tau_1$ and $\tau_2$ correspond to the pathways associated the $V_{HH}$ and $V_{LL}$, respectively. The TT population of Dimer AD, ac, bc and cd with S-shape were fitted by Heaviside step function $P$ (TT) = $a/(1 + e^{-w(t-t0)})$, where $t_0$ is the time at which the TT population reaches the half. In this case, the SF rate can be written as $1/t_0$.

Results show that in **DPND** system, the face-to-face dimer ab features ultrafast TT population via CT state with a SF rate of 62.7 ps$^{-1}$, while all non-nearest neighbor dimer ac, ad, and cd exhibit the relatively slower SF process with much smaller rate constant of about 1 ps$^{-1}$ due to the smaller electronic couplings. That is, only the H-type aggregation dimer ab plays a key role in SF process for **DPND** system. In **DPND6** system, besides the face-to-face dimer AB displaying a SF rate of 12.3 ps$^{-1}$, the non-nearest neighbor dimer AC, and AD also present SF potential with rate constants of 6.9 and 1.3 ps$^{-1}$, respectively. Dimer BD shows no any TT population given the substantially smaller electronic coupling. These results also elucidate that the relative high CT energy in the non-nearest neighbor dimer ac, ad, cd, AC, and AD render no CT population in the SF process. Therefore it is expected that the SF dynamics won't be remarkably fast. CT state might have some

vital impacts on SF dynamics in the studied system, especially for H-type-like aggregation.

**6.4 Intermolecular Slip Displacement Effect.**

Then we have performed theoretical calculations to check the slip displacement effect. **Figure S9** shows how the energy of intermolecular CT state, and the electronic couplings among the localized singlet (SE), CT and TT states ($V_{ex}$, $V_{HH}$, $V_{LL}$, $V_{HL}$ and $V_{LH}$) vary with lateral slip distance (ΔX) and longitudinal slip distance (ΔY) for dimer ab of DPND system. It is obvious that the CT state could be stabilized at very small intermolecular displacements, which further verifies our conclusion that the distinctive H-type-like aggregation of current DPND system could substantially stabilize CT state and make it close in energy with singlet, and excimer, as well as subsequent TT states to facilitate mixing and conversion process of these excited state species.

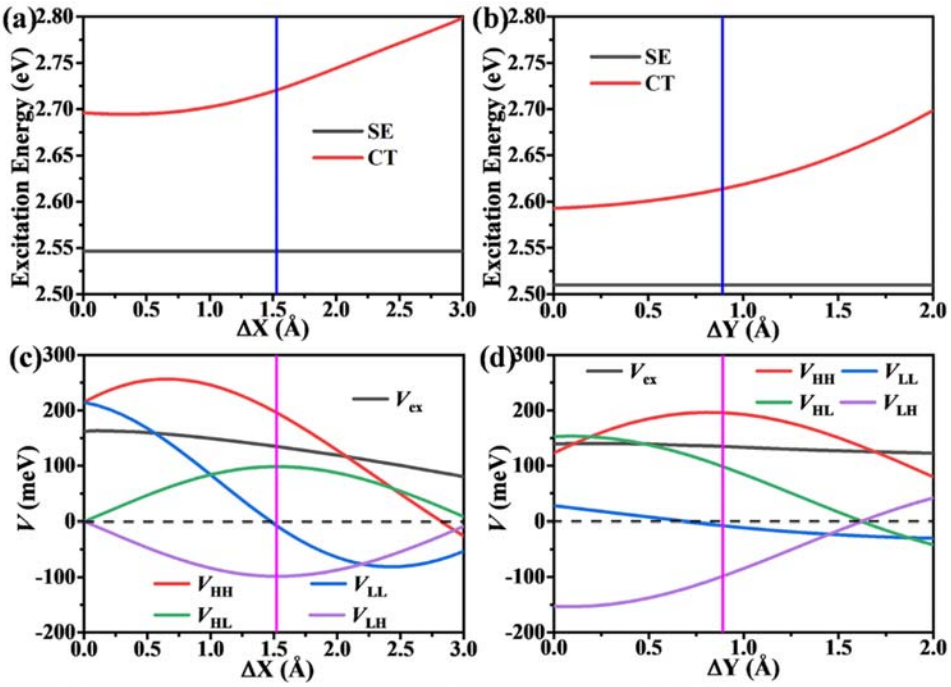


**Figure S9**. Calculated CT state energy vs a) lateral slip distance (ΔX) and b) longitudinal slip distance (ΔY) of DPND dimer system. Calculated electron couplings $V_{ex}$, $V_{HH}$, $V_{LL}$, $V_{HL}$ and $V_{LH}$ vs c) lateral slip distance (ΔX), and d) longitudinal slip distance (ΔY) of DPND dimer system.

In the current molecular packing of ab (ΔX = 1.52 Å in the crystal structure of DPND), the electronic couplings between two CT states and TT state ($|V_{HL}|$ and $|V_{LH}|$) reach the mixima, which is of advantage to the population transfer from the CT to TT states. When ΔX = 1.52 Å is fixed and

ΔY is changed, $V_{HH}$ reaches the miximum value in current molecular packing, which is of advantage to the population transfer from SE to CT states. Meantime, we observe that with the current packing of ab, the exciton-exciton coupling $V_{ex}$ only holds a medium value, indicating that there is no strong SE-SE coherent motion, which can be easily breaken by the electron–phonon coupling (see section 6.6 for details). We thus deduce that the current intermolecular packing of H-type-like aggregation dimer ab in DPND system turns out to be the optimal molecular arrangement for the maximum SF rate.

**6.5 Effective Couplings from SE to TT States.**

To further elucidate the mechanism which gives rise to the difference in SF rates for the studied dimers, we map the above five-configuration Hamiltonian into an effective Hamiltonian with three-configurations of interest[19] with respect to the eigenvalue partition technique.[21] For the CT-mediated SF process of the dimer system, the corresponding eigenvalue equation with five diabatic states can be written as[4]

$$\begin{pmatrix} E_{S_1S_0}-E & V_{ex} & V_{LL} & V_{HH} & 0 \\ V_{ex} & E_{S_0S_1}-E & V_{HH} & V_{LL} & 0 \\ V_{LL} & V_{HH} & E_{CA}-E & 0 & V_{LH} \\ V_{HH} & V_{LL} & 0 & E_{AC}-E & V_{HL} \\ 0 & 0 & V_{LH} & V_{HL} & E_{TT}-E \end{pmatrix} \begin{pmatrix} c_1 \\ c_2 \\ c_3 \\ c_4 \\ c_5 \end{pmatrix} = 0 \qquad \textbf{(S17)}$$

By partitioning the 5-configuration eigenvalue problem, we may convert it into an eigenvalue problem with three configurations of interest, including $S_1S_0$, $S_0S_1$ and TT. We have **eq S18** and **S19**,

$$\begin{aligned} &\left(E_{S_1S_0}-E\right)c_1 + V_{ex}c_2 + V_{LL}c_3 + V_{HH}c_4 = 0 \\ &V_{ex}c_1 + \left(E_{S_1S_0}-E\right)c_2 + V_{HH}c_3 + V_{LL}c_4 = 0 \\ &V_{LH}c_3 + V_{HL}c_4 + \left(E_{TT}-E\right)c_5 = 0 \end{aligned} \qquad \textbf{(S18)}$$

and

$$c_3 = \frac{V_{\mathrm{LL}}c_1 + V_{\mathrm{HH}}c_2 + V_{\mathrm{LH}}c_5}{E - E_{\mathrm{CA}}}$$
$$c_4 = \frac{V_{\mathrm{HH}}c_1 + V_{\mathrm{LL}}c_2 + V_{\mathrm{HL}}c_5}{E - E_{\mathrm{AC}}} \quad \textbf{(S19)}$$

Substituting **eq S19** into **eq S18** yields

$$\begin{pmatrix} E_{\mathrm{S_1S_0}} + \frac{V_{\mathrm{LL}}V_{\mathrm{LL}}}{E-E_{\mathrm{CA}}} + \frac{V_{\mathrm{HH}}V_{\mathrm{HH}}}{E-E_{\mathrm{AC}}} - E & V_{\mathrm{ex}} + \frac{V_{\mathrm{LL}}V_{\mathrm{HH}}}{E-E_{\mathrm{CA}}} + \frac{V_{\mathrm{HH}}V_{\mathrm{LL}}}{E-E_{\mathrm{AC}}} & \frac{V_{\mathrm{LL}}V_{\mathrm{LH}}}{E-E_{\mathrm{CA}}} + \frac{V_{\mathrm{HH}}V_{\mathrm{HL}}}{E-E_{\mathrm{AC}}} \\ V_{\mathrm{ex}} + \frac{V_{\mathrm{HH}}V_{\mathrm{LL}}}{E-E_{\mathrm{CA}}} + \frac{V_{\mathrm{LL}}V_{\mathrm{HH}}}{E-E_{\mathrm{AC}}} & E_{\mathrm{S_1S_0}} + \frac{V_{\mathrm{HH}}V_{\mathrm{HH}}}{E-E_{\mathrm{CA}}} + \frac{V_{\mathrm{LL}}V_{\mathrm{LL}}}{E-E_{\mathrm{AC}}} - E & \frac{V_{\mathrm{HH}}V_{\mathrm{LH}}}{E-E_{\mathrm{CA}}} + \frac{V_{\mathrm{LL}}V_{\mathrm{HL}}}{E-E_{\mathrm{AC}}} \\ \frac{V_{\mathrm{LH}}V_{\mathrm{LL}}}{E-E_{\mathrm{CA}}} + \frac{V_{\mathrm{HL}}V_{\mathrm{HH}}}{E-E_{\mathrm{AC}}} & \frac{V_{\mathrm{LH}}V_{\mathrm{HH}}}{E-E_{\mathrm{CA}}} + \frac{V_{\mathrm{HL}}V_{\mathrm{LL}}}{E-E_{\mathrm{AC}}} & E_{\mathrm{TT}} + \frac{V_{\mathrm{LH}}V_{\mathrm{LH}}}{E-E_{\mathrm{CA}}} + \frac{V_{\mathrm{HL}}V_{\mathrm{HL}}}{E-E_{\mathrm{AC}}} - E \end{pmatrix} \begin{pmatrix} c_1 \\ c_2 \\ c_5 \end{pmatrix} = 0 \quad \textbf{(S20)}$$

Therefore, the Hamiltonian with three configurations of interest can be written as

$$\begin{pmatrix} \tilde{E}_{\mathrm{S_1S_0}} & \tilde{V}_{\mathrm{ex}} & \tilde{V}_1 \\ \tilde{V}_{\mathrm{ex}} & \tilde{E}_{\mathrm{S_1S_0}} & \tilde{V}_2 \\ \tilde{V}_1 & \tilde{V}_2 & \tilde{E}_{\mathrm{TT}} \end{pmatrix} \quad \textbf{(S21)}$$

The calculated effective Hamiltonian for ab and AB with three configurations of interest can thus be written as **eq S22** and **S23**.

$$H_{\mathrm{ab}}^{eff} = \begin{pmatrix} 2443.2 & 139.9 & -34.8 \\ 139.9 & 2443.2 & 34.8 \\ -34.8 & 34.8 & 2047.0 \end{pmatrix} \quad \textbf{(S22)}$$

$$H_{\mathrm{AB}}^{eff} = \begin{pmatrix} 2543.4 & 99.0 & 7.8 \\ 99.0 & 2543.4 & -7.8 \\ 7.8 & -7.8 & 2364.0 \end{pmatrix} \quad \textbf{(S23)}$$

**6.6 SF Dynamics in One-Dimensional Molecular Chain.**

Due to the strong exciton coupling, it is necessary to consider SF dynamics beyond the aforementioned dimer systems. Given the exciton-exciton coupling exerts mainly in the face-to-face stacking directions, we construct a one-dimensional molecular chain along this direction to observe SF dynamics in aggregates (**Figure S10**). Results show that SF rates for **DPND6** are proportional to the number of monomers, while these for **DPND** will decrease at first and then increase with aggregate size, which can be attributed to the difficulty for the electron-phonon

coupling to break the coherent motions associated with strong electronic coupling. Then we use the coherence participation ratio (CPR) to describe the coherence of SE states (**Figure S11**). The CPR of SE states in **DPND6** system is inversely proportional to the number of monomers after 25 fs. Due to the stronger $V_{ex}$, the strength of coherence in **DPND** system will increase with aggregate size. On the whole, the stronger electronic coupling has the main contribution to the larger SF rate in **DPND** system. But it should be borne in mind that the oversize electronic coupling may not benefit to SF process.

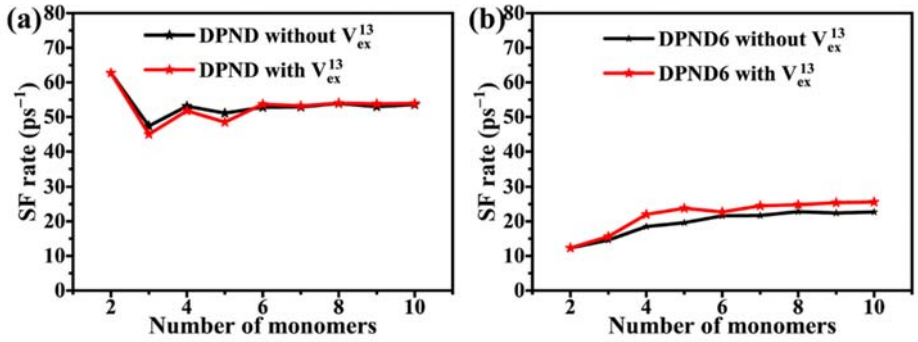


**Figure S10**. SF rates in terms of molecular chain length for **DPND** and **DPND6** system.

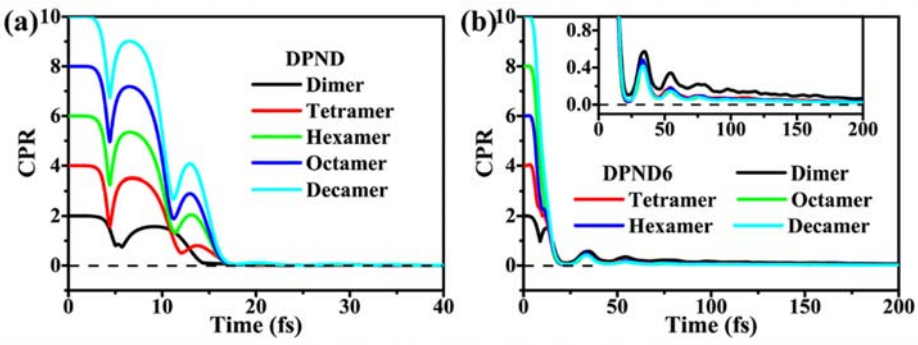


**Figure S11**. CPR of SE states in terms of molecular chain length for **DPND** and **DPND6** systems.

### 6.7 The Calculated Vertical Excitation Energies.

The vertical excitation energies for monomer and dimer units were calculated by TDDFT/PCM method to present clearer evidence of H-type-like aggregation in current **DPND** and **DPND6** systems (**Table S2**). Results show that in both dimer unit ab and AB, $S_1$ state exhibits an oscillator strength of zero, while the higher excited electronic states (i.e. $S_2$ and $S_4$) feature obvious

non-zero oscillator strengths, which clearly indicate the H-type aggregation behaviour in current studied system. Due to the strong mixing between the molecular localized SE and intermolecular CT states in dimer ab of **DPND**, the oscillator strengths of $S_2$ and $S_4$ states are nearly same and are smaller than that of the monomer's $S_1$ state. This is different from the conventional H-type aggregation where the intermolecular CT states doesn't contribute obviously to the low-lying adiabatic excited states, leading to $S_2$ state of dimer possessing a twice of oscillator strength of the monomer's $S_1$ state. With respect to the calculated excitation energies, we deduce that the low-energy wide absorption band of **DPND** thin film around 400-550 nm (**Figure 3b** in main text) is originated from the strong mixing between lowest-lying SE and CT states, and the absorption tail at the long wavelength around 600 nm is assigned to the vibronic coupling effect in the lowest excited state (corresponding to a dipole-forbidden transition). By contrast, **DPND6** system is less influenced by CT states as confirmed by the aforementioned calculated results.

**Table S2**. The calculated vertical excitation energy ($\Delta E$/eV) and oscillator strength (f) for monomer and dimer units in **DPND** and **DPND6** systems by TDDFT/PCM.

| Excited State | DPND | | DPND6 | |
|---|---|---|---|---|
| | **Monomer** | **Dimer ab** | **Monomer** | **Dimer AB** |
| **$S_1$** | 2.3092 (0.7004) | 2.1931 (0.0000) | 2.3521 (0.6251) | 2.3967 (0.0000) |
| **$S_2$** | 3.1782 (0.0000) | 2.3623 (0.5860) | 3.2249 (0.0000) | 2.5975 (0.9264) |
| **$S_3$** | 3.7237 (0.0000) | 2.7596 (0.0000) | 3.6621 (0.0000) | 2.7147 (0.0000) |
| **$S_4$** | 3.8288 (0.0000) | 2.8724 (0.5565) | 3.6779 (0.0023) | 2.7331 (0.0799) |
| **$S_5$** | | 3.2041 (0.0003) | | 3.2487 (0.0003) |
| **$S_6$** | | 3.2305 (0.0000) | | 3.2661 (0.0000) |
| **$S_7$** | | 3.6435 (0.0000) | | 3.6983 (0.0000) |
| **$S_8$** | | 3.7652 (0.0019) | | 3.7091 (0.0010) |

## 7. Supplementary Data for TA Measurements in Thin Film.

### 7.1 Heat Effect Elimination.

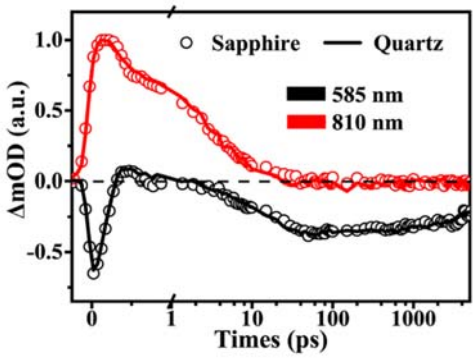


**Figure S12**. Normalized kinetic profiles for thin films deposited on sapphire and quartz substrates upon excitation at 470 nm. Results indicate that the kinetics from fs-TA measurements at 585 and 810 nm show almost no obvious changes between samples on different substrates. Therefore, no strong thermal effects were observed in TA measurement for **DPND** thin films.

### 7.2 Excitation Density and Wavelength Dependence.

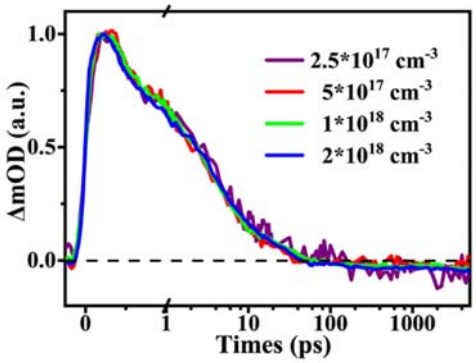


**Figure S13**. Normalized kinetic profiles for thin film upon excitation at 470 nm with different excitation densities. Results show that the excitation density has little impact on the excited-state photophysics in fs-TA measurement for solid films.

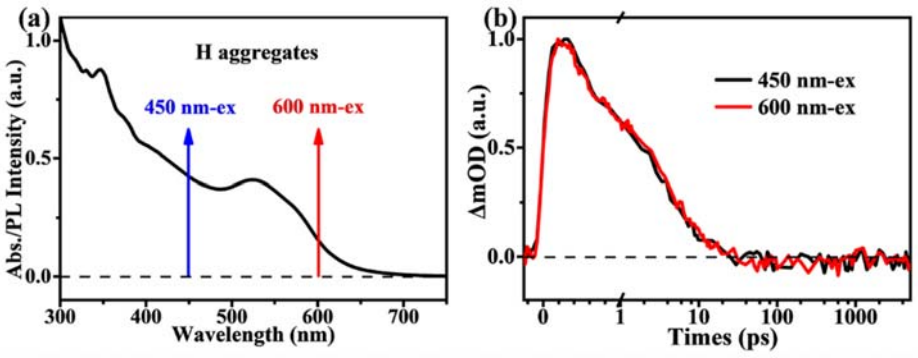


**Figure S14**. a) Steady state absorption spectra of H aggregates of **DPND** system including the excitation wavelengths in TA control measurements. b) Normalized kinetic profiles for thin film upon different excitation wavelengths (450 and 600 nm). Results show that the excitation wavelength has little impact on the excited-state photophysics in fs-TA measurement for solid films, which indicate that the long wavelength absorption band tail is not resulting from another different aggregation mode in thin film, such as slip-stacked J-type aggregation.

### 7.3 Supplementary Data for ns-TA measurements.

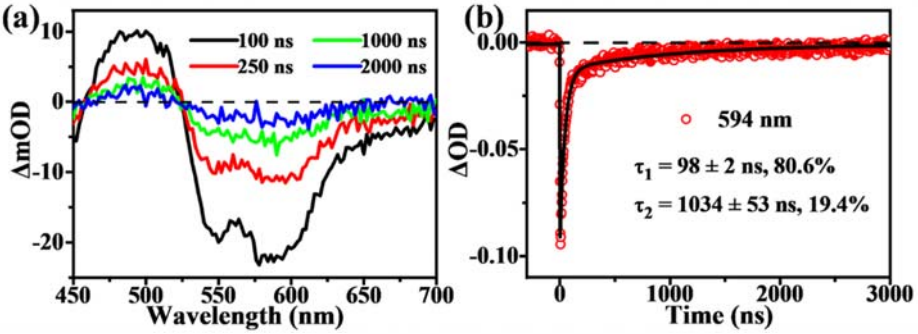


**Figure S15**. a) Selected spectral slices and b) the corresponding decay kinetics from ns-TA measurements for **DPND** thin films following excitation at 532 nm.

### 7.4 Triplet Sensitization in Thin Film.

Triplet sensitization in solid films was performed by blending a small portion (~ 10 mol%) of $PdPc(OBu)_8$ (Pd) into PMMA or **DPND** thin film.[2, 22] Pd was chosen as a sensitizer because it is known to undergo rapid (picosecond) intersystem crossing with quantitative triplet yield.[23] Then fs-TA measurements were performed by selectively exciting the Pd molecules in PMMA film or doped **DPND** thin film at 760 nm (**Figure S16**). Based on the obtained TA data, we used a previously described methodology to extract the TA spectral component arising from **DPND** triplets ($T_1$).[2, 22-24] As shown in **Figure S16b**, the derived sensitized triplet spectra are in blue, by

taking the difference between the Pd triplet in PMMA (black) and the **DPND** triplets in Pd (red) at 1 ns which were carefully adjusted to align the red edge (650-680 nm) of the PMMA and **DPND** spectra. The ΔOD sensitized spectrum therefore represents the overlap of the triplet ESA and the GSB signal. The experimental long-lived $T_1$ curves from pure **DPND** films are also overlaid in pink dash lines. The sensitized triplet line shapes (blue) overlap well with the TA spectral signatures (pink dash lines), which confirms the dominant end species formed following photo-excitation are undoubtedly long-lived free triplets.

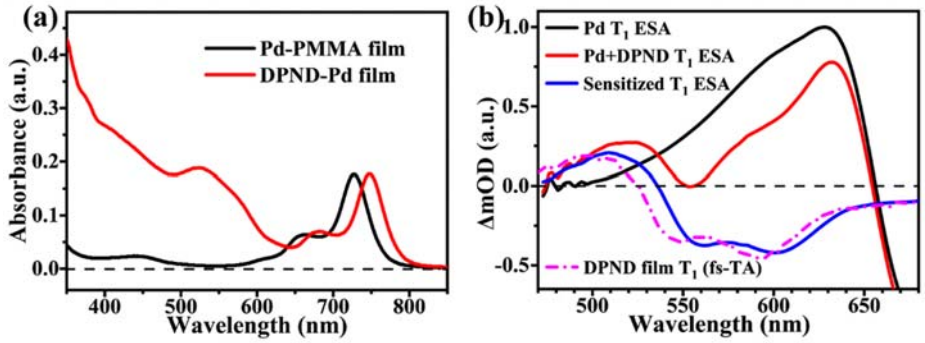


**Figure S16.** a) Steady state absorption of Pd-PMMA and **DPND**-Pd doped films. b) Sensitized triplet spectra for **DPND** thin films.

### 7.5 Triplet Yield Determination.

Triplet yields were calculated with a method previously reported by Wasielewski et al. based on quantifying GSB signal in ns-TA data and relating this exciton density to the calculated exciton density due to the laser power, spot size, and the film thickness and absorption.[4, 22, 25]

These values were used to calculate an excitation density:

$$\xi = \frac{E \cdot \lambda \cdot K \cdot (1 - 10^{-A})}{l \cdot a}$$

As well as number density:

$$No.Density = \frac{Z}{V}$$

The ratio of which ($\xi$/***No. Density***) gives a scaling factor for the ground state absorption spectrum that produces the amount of GSB at $t_0$ or with 100% triplet yield. We then examine the

actual bleach necessary to produce the pure triplet absorption spectrum from the ns-TA spectra and compare this to the calculated bleach. To more strictly quantify this analysis we can focus on a region where the GSB spectrum is strongly featured. As outlined by Carmichael and Hug,[26] addition of the ground state absorption spectrum to the transient trace so as to remove the minimum at this position yields a reasonable triplet-triplet absorption spectrum (**Figure S17**).

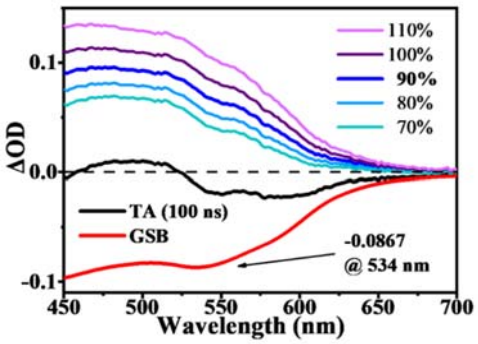


**Figure S17**. Triplet-triplet absorption spectra. Spectra are created by addition of scaled GSB (red) to the 100 ns ns-TA spectrum (black).

These traces then give approximate measure of the GSB addition necessary to obtain a purely triplet-triplet spectrum and, thus, the triplet yield. The amount of GSB necessary to produce a linear trace in this region is used as the yield. The experimental error is derived from these traces as these errors are found to be greater than the error from measurement uncertainties. As the yield is determined from a 100 ns TA trace, a portion of the triplet population has decayed as a result of triplet-triplet annihilation. To correct for this, the yield is extrapolated to $t_0$ using the triplet annihilation kinetics:

$$\boldsymbol{TY\%} = \boldsymbol{TY\%_{100\,ns}} \cdot \frac{\mathbf{1}}{\boldsymbol{A_1 \cdot e^{-100/\tau_1} + A_2 \cdot e^{-100/\tau_2}}}$$

## 8. References


1. Wang, L.; Lin, L.; Yang, J.; Wu, Y.; Wang, H.; Zhu, J.; Yao, J.; Fu, H., Singlet Fission in a Pyrrole-Fused Cross-Conjugated Skeleton with Adaptive Aromaticity. *J. Am. Chem. Soc.* **2020,** *142*, 10235-10239.

2. Wang, L.; Zhang, T.-S.; Fu, L.; Xie, S.; Wu, Y.; Cui, G.; Fang, W.-H.; Yao, J.; Fu, H., High-Lying $3^1A_g$ Dark-State-Mediated Singlet Fission. *J. Am. Chem. Soc.* **2021,** *143*, 5691-5697.

3. Mauck, C. M.; Hartnett, P. E.; Margulies, E. A.; Ma, L.; Miller, C. E.; Schatz, G. C.; Marks, T. J.; Wasielewski, M. R., Singlet Fission via an Excimer-Like Intermediate in 3,6-Bis(Thiophen-2-yl)Diketopyrrolopyrrole Derivatives. *J. Am. Chem. Soc.* **2016,** *138*, 11749-11761.

4. Margulies, E. A.; Logsdon, J. L.; Miller, C. E.; Ma, L.; Simonoff, E.; Young, R. M.; Schatz, G. C.; Wasielewski, M. R., Direct Observation of a Charge-Transfer State Preceding High-Yield Singlet Fission in Terrylenediimide Thin Films. *J. Am. Chem. Soc.* **2017,** *139*, 663-671.

5. Grzybowski, M.; Deperasińska, I.; Chotkowski, M.; Banasiewicz, M.; Makarewicz, A.; Kozankiewicz, B.; Gryko, D. T., Dipyrrolonaphthyridinediones – Structurally Unique Cross-Conjugated Dyes. *Chem. Commun.* **2016,** *52*, 5108-5111.

6. Adamo, C.; Barone, V., Toward Reliable Density Functional Methods without Adjustable Parameters: The PBE0 Model. *J. Chem. Phys.* **1999,** *110*, 6158-6170.

7. Grimme, S.; Antony, J.; Ehrlich, S.; Krieg, H., A Consistent and Accurate ab initio Parametrization of Density Functional Dispersion Correction (DFT-D) for the 94 Elements H-Pu. *J. Chem. Phys.* **2010,** *132*, 154104.

8. Grimme, S.; Ehrlich, S.; Goerigk, L., Effect of the Damping Function in Dispersion Corrected Density Functional Theory. *J. Comput. Chem.* **2011,** *32*, 1456-1465.

9. Frisch, M. J.; Trucks, G. W.; Schlegel, H. B.; Scuseria, G. E.; Robb, M. A.; Cheeseman, J. R.; Scalmani, G.; Barone, V.; Petersson, G. A.; Nakatsuji, H.; Li, X.; Caricato, M.; Marenich, A. V.; Bloino, J.; Janesko, B. G.; Gomperts, R.; Mennucci, B.; Hratchian, H. P.; Ortiz, J. V.; Izmaylov, A. F.; Sonnenberg, J. L.; Williams-Young, D.; Ding, F.; Lipparini, F.; Egidi, F.; Goings, J.; Peng, B.; Petrone, A.; Henderson, T.; Ranasinghe, D.; Zakrzewski, V. G.; Gao, J.; Rega, N.; Zheng, G.;

Liang, W.; Hada, M.; Ehara, M.; Toyota, K.; Fukuda, R.; Hasegawa, J.; Ishida, M.; Nakajima, T.; Honda, Y.; Kitao, O.; Nakai, H.; Vreven, T.; Throssell, K.; Montgomery, J. A.; Jr., P., J. E.; Ogliaro, F.; Bearpark, M. J.; Heyd, J. J.; Brothers, E. N.; Kudin, K. N.; Staroverov, V. N.; Keith, T. A.; Kobayashi, R.; Normand, J.; Raghavachari, K.; Rendell, A. P.; Burant, J. C.; Iyengar, S. S.; Tomasi, J.; Cossi, M.; Millam, J. M.; Klene, M.; Adamo, C.; Cammi, R.; Ochterski, J. W.; Martin, R. L.; Morokuma, K.; Farkas, O.; Foresman, J. B.; Fox, D. J., Gaussian, Inc., Wallingford CT, Gaussian 16. *2016*.

10. El Bakouri, O.; Smith, J. R.; Ottosson, H., Strategies for Design of Potential Singlet Fission Chromophores Utilizing a Combination of Ground-State and Excited-State Aromaticity Rules. *J. Am. Chem. Soc.* **2020,** *142*, 5602-5617.

11. Rohrdanz, M. A.; Herbert, J. M., Simultaneous Benchmarking of Ground- and Excited-State Properties with Long-Range-Corrected Density Functional Theory. *J. Chem. Phys.* **2008,** *129*, 034107.

12. Sun, H.; Hu, Z.; Zhong, C.; Chen, X.; Sun, Z.; Brédas, J.-L., Impact of Dielectric Constant on the Singlet–Triplet Gap in Thermally Activated Delayed Fluorescence Materials. *J. Phys. Chem. Lett.* **2017,** *8*, 2393-2398.

13. Nayak, P. K.; Periasamy, N., Calculation of Ionization Potential of Amorphous Organic Thin-Films Using Solvation Model and DFT. *Org. Electron.* **2009,** *10*, 532-535.

14. Lu, T.; Chen, F., Multiwfn: A Multifunctional Wavefunction Analyzer. *J. Comput. Chem.* **2012,** *33*, 580-592.

15. Wang, Y.-C.; Feng, S.; Liang, W.; Zhao, Y., Electronic Couplings for Photoinduced Charge Transfer and Excitation Energy Transfer Based on Fragment Particle–Hole Densities. *J. Phys. Chem. Lett.* **2021,** *12*, 1032-1039.

16. te Velde, G.; Bickelhaupt, F. M.; Baerends, E. J.; Fonseca Guerra, C.; van Gisbergen, S. J. A.; Snijders, J. G.; Ziegler, T., Chemistry with ADF. *J. Comput. Chem.* **2001,** *22*, 931-967.

17. Zhao, Y.; Liang, W., Charge Transfer in Organic Molecules for Solar Cells: Theoretical Perspective. *Chem. Soc. Rev.* **2012,** *41*, 1075-1087.

18. Zhong, X.; Zhao, Y., Charge Carrier Dynamics in Phonon-Induced Fluctuation Systems from Time-Dependent Wavepacket Diffusion Approach. *J. Chem. Phys.* **2011,** *135*, 134110.

19. Zang, H.; Zhao, Y.; Liang, W., Quantum Interference in Singlet Fission: J- and H-Aggregate Behavior. *J. Phys. Chem. Lett.* **2017,** *8*, 5105-5112.

20. Zang, H.; Ke, Y.; Zhao, Y.; Liang, W., Effects of Charge Transfer State and Exciton Migration on Singlet Fission Dynamics in Organic Aggregates. *J. Phys. Chem. C* **2016,** *120*, 13351-13359.

21. Larsson, S., Electron Transfer in Chemical and Biological Systems. Orbital Rules for Nonadiabatic Transfer. *J. Am. Chem. Soc.* **1981,** *103*, 4034-4040.

22. Hartnett, P. E.; Margulies, E. A.; Mauck, C. M.; Miller, S. A.; Wu, Y.; Wu, Y.-L.; Marks, T. J.; Wasielewski, M. R., Effects of Crystal Morphology on Singlet Exciton Fission in Diketopyrrolopyrrole Thin Films. *J. Phys. Chem. B* **2016,** *120*, 1357-1366.

23. Rihter, B. D.; Kenney, M. E.; Ford, W. E.; Rodgers, M. A. J., Synthesis and Photoproperties of Diamagnetic Octabutoxyphthalocyanines with Deep Red Optical Absorbance. *J. Am. Chem. Soc.* **1990,** *112*, 8064-8070.

24. Korovina, N. V.; Das, S.; Nett, Z.; Feng, X. T.; Joy, J.; Haiges, R.; Krylov, A. I.; Bradforth, S. E.; Thompson, M. E., Singlet Fission in a Covalently Linked Cofacial Alkynyltetracene Dimer. *J. Am. Chem. Soc.* **2016,** *138*, 617-627.

25. Eaton, S. W.; Miller, S. A.; Margulies, E. A.; Shoer, L. E.; Schaller, R. D.; Wasielewski, M. R., Singlet Exciton Fission in Thin Films of Tert-Butyl-Substituted Terrylenes. *J. Phys. Chem. A* **2015,** *119*, 4151-4161.

26. Carmichael, I.; Hug, G. L., Triplet–Triplet Absorption Spectra of Organic Molecules in Condensed Phases. *J. Phys. Chem. Ref. Data* **1986,** *15*, 1-250.

**9. Appendix.**

**Table S3. Crystallographic parameters for DPND crystal**.

| **Compound** | **DPND** |
|---|---|
| **CCDC No.** | 2052443 |
| **Empirical formula** | $C_{14}H_8N_2O_2$ |
| **Formula weight** | 236.22 |
| **Temperature/K** | 170.00 |
| **Crystal system** | Monoclinic |
| **Space group** | $P2_1/n$ |
| **a/Å** | 6.6191(2) |
| **b/Å** | 3.79700(10) |
| **c/Å** | 19.9030(5) |
| **α/°** | 90 |
| **β/°** | 94.592(3) |
| **γ/°** | 90 |
| **Volume/Å$^3$** | 498.61(2) |
| **Z** | 2 |
| **$\rho_{calc}$Mg/cm$^3$** | 1.573 |
| **μ/mm$^{-1}$** | 0.890 |
| **F(000)** | 244.0 |
| **Crystal size/mm$^3$** | 0.34 × 0.05 × 0.01 |
| **Radiation** | CuKα (λ = 1.54184) |
| **2Θ range for data collection/°** | 8.914 to 149.856 |
| **Index ranges** | $-7 \leq h \leq 6$, $-4 \leq k \leq 4$, $-24 \leq l \leq 24$ |
| **Reflections collected** | 8690 |
| **Independent reflections** | 995 [$R_{int}$ = 0.0394, $R_{sigma}$ = 0.0221] |
| **Data/restraints/parameters** | 995 / 0 / 82 |
| **Goodness-of-fit on F$^2$** | 1.117 |
| **Final R indexes [I>=2σ (I)]** | $R_1$ = 0.0370, $wR_2$ = 0.0929 |
| **Final R indexes [all data]** | $R_1$ = 0.0403, $wR_2$ = 0.0951 |
| **Largest diff. peak/hole / e Å$^{-3}$** | 0.16/-0.26 |

**NMR Spectra.**

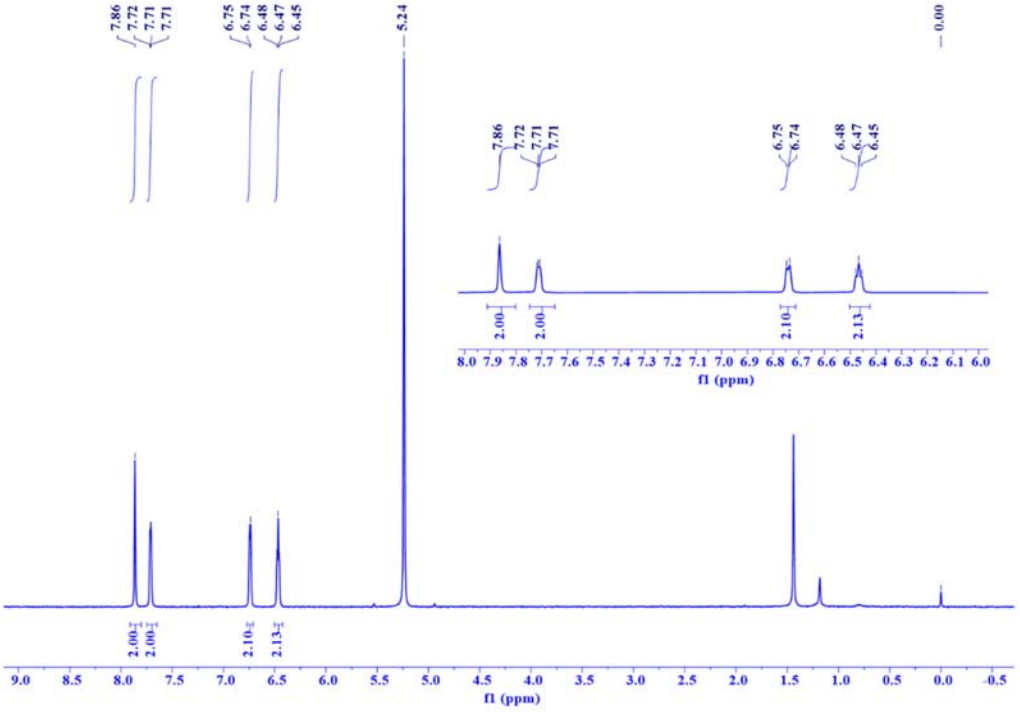


**Figure S18**. $^{1}H$ NMR spectra of **DPND** in $CD_2Cl_2$.

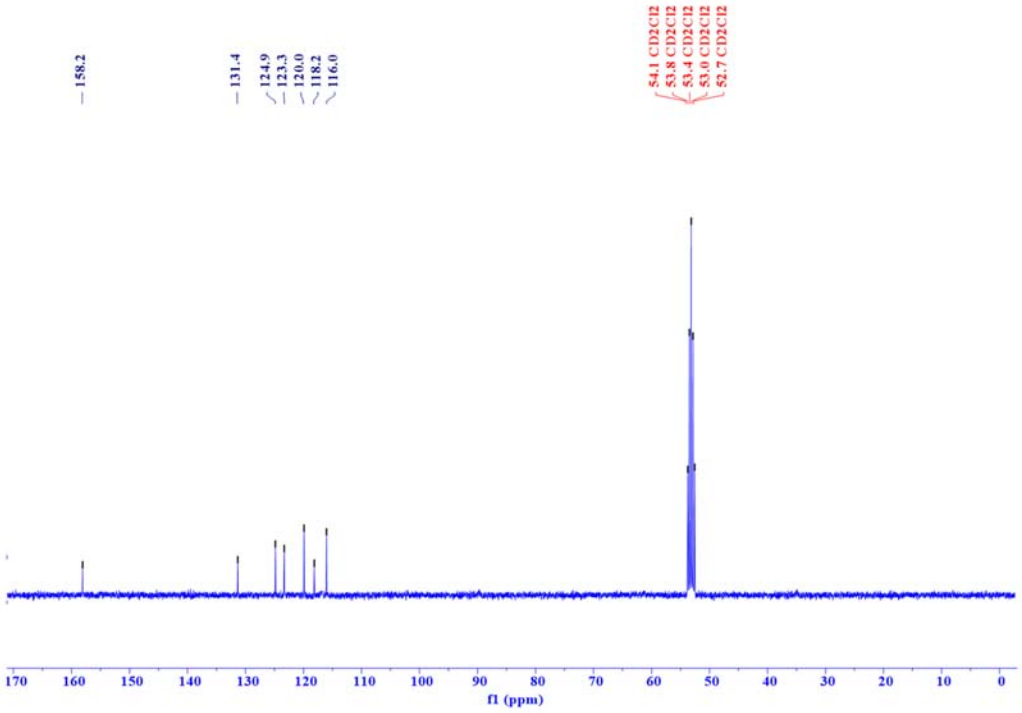


**Figure S19**. $^{13}C$ NMR spectra of **DPND** in $CD_2Cl_2$.

**Table S4. Geometries for All the Optimized Compounds and Transition States.**

| | DPND | | | | | | | | |
|---|---|---|---|---|---|---|---|---|---|
| | $S_0$ | | | $S_1$ | | | $T_1$ | | |
| O | -3.831278 | -0.105747 | 17.832351 | -3.820415 | -0.107729 | 17.852527 | -3.815244 | -0.108554 | 17.856561 |
| O | 0.644416 | 0.105746 | 21.845865 | 0.633553 | 0.107729 | 21.825688 | 0.628383 | 0.108554 | 21.821654 |
| N | -1.781089 | 0.815922 | 17.485557 | -1.769791 | 0.817351 | 17.492559 | -1.765110 | 0.816487 | 17.498745 |
| N | -1.405773 | -0.815921 | 22.192659 | -1.417070 | -0.817352 | 22.185656 | -1.421752 | -0.816488 | 22.179470 |
| C | -0.925658 | 0.177647 | 20.050848 | -0.940540 | 0.174393 | 20.044075 | -0.950049 | 0.171216 | 20.042916 |
| C | -2.261204 | -0.177647 | 19.627367 | -2.246321 | -0.174396 | 19.634139 | -2.236812 | -0.171216 | 19.635299 |
| C | -0.075419 | 0.825583 | 19.202838 | -0.055861 | 0.841344 | 19.181339 | -0.051020 | 0.846034 | 19.173072 |
| C | -3.111442 | -0.825583 | 20.475377 | -3.131000 | -0.841346 | 20.496875 | -3.135842 | -0.846034 | 20.505144 |
| C | -0.494046 | 1.156145 | 17.898644 | -0.473564 | 1.163063 | 17.901313 | -0.472304 | 1.161372 | 17.905901 |
| C | -2.692816 | -1.156145 | 21.779571 | -2.713298 | -1.163064 | 21.776902 | -2.714557 | -1.161372 | 21.772315 |
| C | 0.119737 | 1.793783 | 16.833303 | 0.134627 | 1.810196 | 16.805868 | 0.135212 | 1.812106 | 16.800564 |
| C | -3.306598 | -1.793784 | 22.844912 | -3.321489 | -1.810196 | 22.872348 | -3.322074 | -1.812106 | 22.877652 |
| C | -0.808796 | 1.836952 | 15.768303 | -0.796727 | 1.842612 | 15.765527 | -0.796305 | 1.844187 | 15.762491 |
| C | -2.378066 | -1.836952 | 23.909912 | -2.390135 | -1.842610 | 23.912689 | -2.390557 | -1.844187 | 23.915725 |
| C | -1.966919 | 1.230779 | 16.193412 | -1.962153 | 1.228726 | 16.202868 | -1.959935 | 1.230927 | 16.199791 |
| C | -1.219943 | -1.230778 | 23.484804 | -1.224710 | -1.228725 | 23.475347 | -1.226927 | -1.230927 | 23.478424 |
| C | -2.732580 | 0.150118 | 18.277258 | -2.712899 | 0.154141 | 18.288317 | -2.705908 | 0.156604 | 18.287093 |
| C | -0.454282 | -0.150118 | 21.400957 | -0.473961 | -0.154145 | 21.389897 | -0.480953 | -0.156605 | 21.391122 |
| H | 0.923452 | 1.087192 | 19.530488 | 0.938487 | 1.095616 | 19.523470 | 0.941880 | 1.099026 | 19.517589 |
| H | -4.110313 | -1.087192 | 20.147727 | -4.125348 | -1.095618 | 20.154745 | -4.128742 | -1.099026 | 20.160626 |
| H | 1.127999 | 2.180719 | 16.837732 | 1.141500 | 2.200313 | 16.801324 | 1.141799 | 2.202246 | 16.795031 |
| H | -4.314860 | -2.180721 | 22.840483 | -4.328362 | -2.200312 | 22.876891 | -4.328660 | -2.202246 | 22.883185 |
| H | -0.649246 | 2.266485 | 14.790952 | -0.653128 | 2.267787 | 14.783279 | -0.652398 | 2.269612 | 14.780666 |
| H | -2.537616 | -2.266485 | 24.887263 | -2.533735 | -2.267783 | 24.894938 | -2.534464 | -2.269612 | 24.897549 |
| H | -2.908994 | 1.053534 | 15.700489 | -2.905573 | 1.049253 | 15.712488 | -2.904315 | 1.050424 | 15.712962 |
| H | -0.277867 | -1.053533 | 23.977727 | -0.281290 | -1.049252 | 23.965728 | -0.282547 | -1.050424 | 23.965253 |

**DPND6**

| | $S_0$ | | | $S_1$ | | | $T_1$ | | |
|---|---|---|---|---|---|---|---|---|---|
| O | 7.269351 | 4.412898 | -0.747911 | 7.255218 | 4.386322 | -0.765825 | 7.237840 | 4.411740 | -0.773671 |
| O | 1.725381 | 2.497707 | 0.747957 | 1.739448 | 2.524265 | 0.765787 | 1.756896 | 2.498844 | 0.773711 |
| N | 6.772188 | 3.003813 | 0.933230 | 6.765559 | 2.995669 | 0.934172 | 6.769926 | 2.994299 | 0.909234 |
| N | 2.222551 | 3.906769 | -0.933198 | 2.229100 | 3.914940 | -0.934197 | 2.224815 | 3.916266 | -0.909206 |
| C | 8.055476 | 2.839007 | 1.380188 | 8.052395 | 2.828914 | 1.369413 | 8.069694 | 2.827079 | 1.332398 |
| C | 0.939257 | 4.071612 | -1.380129 | 0.942269 | 4.081651 | -1.369471 | 0.925043 | 4.083521 | -1.332343 |
| C | 8.027257 | 1.946730 | 2.424641 | 8.032032 | 1.938530 | 2.430545 | 8.062986 | 1.931474 | 2.387039 |
| C | 0.967477 | 4.963902 | -2.424571 | 0.962634 | 4.972010 | -2.430624 | 0.931749 | 4.979146 | -2.386968 |
| C | 6.685985 | 1.546772 | 2.615530 | 6.708650 | 1.544710 | 2.647214 | 6.744163 | 1.533398 | 2.616744 |
| C | 2.308753 | 5.363835 | -2.615477 | 2.286011 | 5.365853 | -2.647278 | 2.250575 | 5.377204 | -2.616686 |
| C | 5.910777 | 2.213773 | 1.677286 | 5.904842 | 2.212846 | 1.697853 | 5.920077 | 2.207018 | 1.677369 |
| C | 3.083963 | 4.696810 | -1.677251 | 3.089816 | 4.697753 | -1.697888 | 3.074665 | 4.703555 | -1.677334 |
| C | 6.395083 | 3.825392 | -0.139573 | 6.383535 | 3.803940 | -0.139095 | 6.380495 | 3.809352 | -0.145892 |
| C | 2.599658 | 3.085159 | 0.139580 | 2.611121 | 3.106714 | 0.139104 | 2.614249 | 3.101179 | 0.145891 |
| C | 4.516785 | 2.217541 | 1.405574 | 4.536210 | 2.208980 | 1.439298 | 4.559613 | 2.199017 | 1.441216 |
| C | 4.477959 | 4.693018 | -1.405556 | 4.458444 | 4.701650 | -1.439313 | 4.435132 | 4.711533 | -1.441198 |
| C | 4.042879 | 3.043349 | 0.401146 | 4.054485 | 3.057394 | 0.396807 | 4.064537 | 3.060888 | 0.392856 |
| C | 4.951863 | 3.867198 | -0.401139 | 4.940171 | 3.853255 | -0.396805 | 4.930206 | 3.849647 | -0.392851 |
| C | 3.680889 | 1.337081 | 2.284913 | 3.687362 | 1.339016 | 2.313425 | 3.712593 | 1.329505 | 2.323039 |
| C | 5.313861 | 5.573475 | -2.284893 | 5.307286 | 5.571610 | -2.313449 | 5.282155 | 5.581046 | -2.323016 |
| C | 3.112146 | 2.097632 | 3.486979 | 3.114712 | 2.094772 | 3.518587 | 3.126877 | 2.089810 | 3.515884 |
| C | 5.882546 | 4.812940 | -3.486997 | 5.879992 | 4.815829 | -3.518568 | 5.867820 | 4.820760 | -3.515899 |
| C | 2.255134 | 1.207433 | 4.373633 | 2.248386 | 1.203631 | 4.395271 | 2.253422 | 1.203988 | 4.390913 |
| C | 6.739574 | 5.703133 | -4.373641 | 6.746306 | 5.706969 | -4.395266 | 6.741284 | 5.706583 | -4.390919 |
| C | 1.691176 | 1.937295 | 5.584261 | 1.682914 | 1.928153 | 5.608538 | 1.677365 | 1.934143 | 5.595672 |
| C | 7.303474 | 4.973287 | -5.584307 | 7.311835 | 4.982420 | -5.608490 | 7.317289 | 4.976449 | -5.595716 |
| C | 0.824048 | 1.055205 | 6.472672 | 0.806067 | 1.044975 | 6.486388 | 0.793795 | 1.055482 | 6.471160 |
| C | 8.170619 | 5.855371 | -6.472707 | 8.188669 | 5.865596 | -6.486355 | 8.200867 | 5.855110 | -6.471195 |
| C | 0.263992 | 1.794041 | 7.679336 | 0.245023 | 1.778452 | 7.695880 | 0.221962 | 1.795182 | 7.671781 |
| C | 8.730621 | 5.116550 | -7.679406 | 8.749771 | 5.132093 | -7.695803 | 8.772648 | 5.115431 | -7.671854 |
| H | 8.862723 | 3.373193 | 0.906917 | 8.858189 | 3.356273 | 0.885414 | 8.866818 | 3.360280 | 0.841659 |
| H | 0.132009 | 3.537434 | -0.906852 | 0.136478 | 3.554289 | -0.885472 | 0.127917 | 3.550323 | -0.841604 |
| H | 8.884621 | 1.615357 | 2.990723 | 8.899962 | 1.615597 | 2.986155 | 8.937356 | 1.606198 | 2.930616 |
| H | 0.110110 | 5.295299 | -2.990634 | 0.094707 | 5.294912 | -2.986258 | 0.057377 | 5.304446 | -2.930526 |
| H | 6.323061 | 0.852375 | 3.357459 | 6.350517 | 0.864815 | 3.404615 | 6.397291 | 0.846186 | 3.372448 |
| H | 2.671679 | 6.058235 | -3.357403 | 2.644144 | 6.045737 | -3.404689 | 2.597446 | 6.064425 | -3.372382 |
| H | 2.856821 | 0.910386 | 1.715286 | 2.862205 | 0.916990 | 1.741619 | 2.898724 | 0.887730 | 1.750540 |
| H | 6.137958 | 6.000128 | -1.715275 | 6.132414 | 5.993684 | -1.741639 | 6.096050 | 6.022782 | -1.750523 |
| H | 4.302744 | 0.512686 | 2.644252 | 4.300949 | 0.508137 | 2.674876 | 4.333659 | 0.509114 | 2.695172 |

| | | | | | | | | | |
|---|---|---|---|---|---|---|---|---|---|
| H | 4.692025 | 6.397901 | -2.644193 | 4.693680 | 6.402457 | -2.674946 | 4.661104 | 6.401465 | -2.695111 |
| H | 2.511634 | 2.936984 | 3.123540 | 2.520401 | 2.938990 | 3.156090 | 2.534382 | 2.931632 | 3.144794 |
| H | 6.483032 | 3.973552 | -3.123599 | 6.474328 | 3.971648 | -3.156023 | 6.460295 | 3.978908 | -3.144850 |
| H | 3.938860 | 2.521114 | 4.070660 | 3.941412 | 2.510683 | 4.108100 | 3.946734 | 2.511420 | 4.111311 |
| H | 5.055801 | 4.389511 | -4.070673 | 5.053323 | 4.399862 | -4.108083 | 5.047934 | 4.399197 | -4.111321 |
| H | 1.429346 | 0.798569 | 3.777181 | 1.422849 | 0.803844 | 3.792221 | 1.433105 | 0.800416 | 3.783241 |
| H | 7.565394 | 6.111942 | -3.777194 | 7.571813 | 6.106812 | -3.792212 | 7.561628 | 6.110108 | -3.783253 |
| H | 2.847213 | 0.345777 | 4.710965 | 2.833738 | 0.335993 | 4.729154 | 2.836039 | 0.338113 | 4.734379 |
| H | 6.147524 | 6.564825 | -4.710930 | 6.160928 | 6.574570 | -4.729198 | 6.158687 | 6.572488 | -4.734342 |
| H | 1.102020 | 2.799661 | 5.244772 | 1.100649 | 2.796531 | 5.272473 | 1.097452 | 2.800471 | 5.250243 |
| H | 7.892602 | 4.110886 | -5.244859 | 7.894126 | 4.114078 | -5.272377 | 7.897181 | 4.110090 | -5.250329 |
| H | 2.517676 | 2.349180 | 6.179152 | 2.508965 | 2.330694 | 6.210417 | 2.498164 | 2.340537 | 6.202212 |
| H | 6.476943 | 4.561457 | -6.179192 | 6.485815 | 4.579822 | -6.210374 | 6.496461 | 4.570103 | -6.202250 |
| H | -0.000266 | 0.644939 | 5.876002 | -0.018009 | 0.644423 | 5.882819 | -0.024887 | 0.650812 | 5.862986 |
| H | 8.994960 | 6.265587 | -5.876042 | 9.012715 | 6.266205 | -5.882782 | 9.019577 | 6.259732 | -5.863026 |
| H | 1.413809 | 0.193118 | 6.809152 | 1.388768 | 0.176681 | 6.819170 | 1.374257 | 0.189473 | 6.813747 |
| H | 7.580884 | 6.717492 | -6.809149 | 7.605942 | 6.733854 | -6.819186 | 7.620426 | 6.721150 | -6.813740 |
| H | -0.354854 | 2.642036 | 7.368349 | -0.366768 | 2.632777 | 7.388254 | -0.387903 | 2.647261 | 7.354220 |
| H | 9.349439 | 4.268521 | -7.368457 | 9.361588 | 4.277804 | -7.388129 | 9.382492 | 4.263321 | -7.354336 |
| H | -0.354759 | 1.140684 | 8.300823 | -0.381032 | 1.124539 | 8.309446 | -0.408711 | 1.144281 | 8.283831 |
| H | 9.349386 | 5.769902 | -8.300885 | 9.375815 | 5.786006 | -8.309381 | 9.403328 | 5.766331 | -8.283897 |
| H | 1.069373 | 2.187349 | 8.308308 | 1.049864 | 2.161775 | 8.331676 | 1.021115 | 2.182835 | 8.312134 |
| H | 7.925211 | 4.723294 | -8.308373 | 7.944960 | 4.748712 | -8.331603 | 7.973466 | 4.727826 | -8.312201 |